

Strong-coupling dynamics of Bose-Einstein condensate in a double-well trap

V.O. Nesterenko¹, A.N. Novikov¹ and E. Suraud²

¹Bogoliubov Laboratory of Theoretical Physics, Joint Institute for Nuclear Research, Dubna, Moscow region, 141980, Russia

E-mail: nester@theor.jinr.ru

²Laboratoire de Physique Quantique, Université Paul Sabatier, 118 Route de Narbonne, 31062 cedex, Toulouse, France

Abstract. Dynamics of the repulsive Bose-Einstein condensate (BEC) in a double-well trap is explored within the 3D time-dependent Gross-Pitaevskii equation. The model avoids numerous common approximations (two-mode treatment, time-space factorization, fixed values of the chemical potential and barrier penetrability, etc) and thus provides a realistic description of BEC dynamics, including both weak-coupling (sub-barrier) and strong-coupling (above-barrier) regimes and their crossover. The strong coupling regime is achieved by increasing the number N of BEC atoms and thus the chemical potential. The evolution with N of Josephson oscillations (JO) and Macroscopic Quantum Self-Trapping (MQST) is examined and the crucial impact of the BEC interaction is demonstrated. At weak coupling, the calculations well reproduce the JO/MQST experimental data. At strong coupling, with a significant overlap of the left and right BECs, we observe a remarkable persistence of the Josephson-like dynamics: the JO and MQST converge to a high-frequency JO-like mode where both population imbalance and phase difference oscillate around the zero averages. The results open new avenues for BEC interferometry.

PACS numbers: 03.75.Lm, 03.75.Kk

Submitted to: *J. Phys. B: At. Mol. Opt. Phys.*

1. Introduction

The trapped Bose-Einstein condensate (BEC) is nowadays widely recognized as a source of new fascinating physics, see monographs [1, 2] as well as early [3, 4, 5] and recent [6, 7] reviews. Among diverse aspects of this field, a large attention is paid to dynamics of bound condensates and relevant nonlinear effects caused by the interaction between BEC atoms [6, 8]. A boson Josephson junction in a double-well trap represents a typical example of relevant system. Its basic dynamical regimes, Josephson oscillations (JO) and Macroscopic Quantum Self-Trapping (MQST), were widely investigated in the weak coupling limit, both in theory [6, 8, 9, 10] and experiment [11, 12, 13]. Last years, new processes in bound condensates, like controlled BEC transport [14, 15], matter wave interferometry [16], squeezing and entanglement [17], were in the focus. Being diverse and sophisticated, these processes concern, nevertheless, the basic JO and MQST dynamics and, what is important, often occur beyond the weak coupling limit. Thus, the study of JO/MQST at strong coupling (SC), e.g. in the crossover between sub-barrier and above-barrier transfer, becomes essential.

The SC regime routinely arises at a strong interaction or/and large number of BEC atoms. Hence this regime is quite common. At the same time, its features have not been yet properly investigated. Note that at SC, the left and right BECs in a double-well trap are not well separated, so that the use of the ordinary variables of Josephson dynamics, population imbalance z and phase difference θ , is not well justified. There thus arises a general question whether the JO and MQST survive at SC and, if yes, to what extent they are modified?

Numerous previous studies of Josephson dynamics in a double-well trap were performed within the two-mode approximation (TMA) [18], where only two lowest energy levels of the system contribute to the dynamics and a weak coupling of the condensates is assumed. Obviously, SC dynamics can involve many energy levels and the TMA is then not correct. Even the TMA modifications, like a variable tunneling model [19] and a direct implementation of Wannier states [20], do not amend the principle TMA limitation to deal only with two lowest BEC states and thus leave TMA ineligible to the SC case.

The SC dynamics requires a more involved theory embracing impact of all excited states and avoiding, as much as possible, other standard approximations, e.g. the space-time factorization and partition (for every well) of the total order parameter. There are already some studies of this kind [6, 8, 21, 22, 23]. Most of them consider transformation of the trap from a double to a single well shape [21] or back [22, 23] and thus partly concern the SC case. The treatment varies from using the Gross-Pitaevskii equation [24] in [21] to many-body quantum dynamics in [22, 23]. These studies confirm the important role played by the excited states, beyond the TMA. However, these studies do not especially address the evolution of the Josephson dynamics when approaching the SC and do not provide a relevant analysis. Moreover, these studies are usually performed in the one-dimensional (1D) limit [25], the relevance of which is not well

demonstrated for the SC. In addition, the 1D limit is obviously questionable in a true three-dimensional (3D) case, which is often met in practice, see e.g. the JO/MQST Heidelberg experiment [11, 12].

In this paper, we analyze the evolution of the JO/MQST dynamics in a double-well trap while transforming the system from the weak coupling to the SC. The transfer is achieved by increasing the number of BEC atoms from $N=1000$ to 10000. We thus obtain the rise of the cumulative effect of the repulsive interaction and the subsequent upshift of the chemical potential. The analysis is based on an explicit solution of the 3D time-dependent Gross-Pitaevskii equation for the total order parameter. None of the questionable approximations mentioned above is thus used. Both the population imbalance z and phase difference θ are examined.

The calculations are performed for a double-well configuration and the JO/MQST initial conditions of the Heidelberg experiment [11, 12]. For $N=1000$, we reproduce the JO/MQST experimental data [11, 12] for the repulsive condensate of ^{87}Rb atoms. This justifies the relevance of our model in the weak coupling limit. By increasing the number of atoms up to $N=10000$, we approach the SC regime and show that, despite an essential intersection of the left and right BECs in the double-well trap, these BECs still keep their individuality. Hence, using the relative Josephson conjugate variables z and θ remains reasonable. We show that JO survive at SC, though with a higher frequency. The MQST is transformed to a similar JO. Actually, JO and MQST merge to the same mode. Perhaps, a similar MQST \rightarrow JO transfer was earlier predicted for 1D BEC as a reappearance of tunneling in the strong interaction limit [26].

In most of the previous calculations (see, e.g. [8]), the initial conditions are obtained by constraining the system into a non-stationary state of the symmetric trap. This may be questionable at SC. In this respect, we build initial conditions within a more realistic technique [11, 12]. Namely, a stationary state with the proper initial conditions is produced in an asymmetric trap and then the trap is non-adiabatically transformed to the symmetric form.

The paper is organized as follows. The calculation scheme is sketched in Sec. 2. Results of the calculations are discussed in Sec. 3. A summary is given in Sec. 4.

2. Calculation scheme

We solve the 3D time-dependent Gross-Pitaevskii equation [24]

$$i\hbar\frac{\partial\Psi}{\partial t}(\mathbf{r}, t) = \left[-\frac{\hbar^2}{2m}\nabla^2 + V(\mathbf{r}) + g_0|\Psi(\mathbf{r}, t)|^2\right]\Psi(\mathbf{r}, t) \quad (1)$$

for the total order parameter $\Psi(\mathbf{r}, t)$ describing the BEC in both left and right wells of the trap. Here $g_0 = 4\pi\hbar^2 a_s/m$ is the interaction parameter, a_s is the scattering length, and m is the atomic mass. The trap potential

$$V(\mathbf{r}) = \frac{m}{2}(\omega_x^2 x^2 + \omega_y^2 y^2 + \omega_z^2 z^2) + V_0 \cos^2(\pi x/q_0) \quad (2)$$

includes the anisotropic harmonic confinement and the barrier in x -direction, where V_0 is the barrier height and q_0 determines the barrier width. Note that the barrier parameters may depend on time at the stage of preparation of the initial conditions.

Following the experiment [11, 12], we use a BEC of ^{87}Rb atoms with $a_s = 5.75$ nm. The trap frequencies are $\omega_x = 2\pi \times 78$ Hz, $\omega_y = 2\pi \times 66$ Hz, $\omega_z = 2\pi \times 90$ Hz, i.e. $\omega_y + \omega_z = 2\omega_x$ [11, 12]. The barrier parameters are $V_0 = 420 \times h$ Hz and $q_0 = 5.2$ μm [11, 12]. The distance between centers of the left and right wells is then $d = 4.4$ μm . For $N=1000$ atoms, we reproduce the conditions of the JO/MQST Heidelberg experiment [11, 12] for a weak coupling of the left and right BEC fractions through the barrier.

The static solutions of (1) are found within the damped gradient method [27] while the time evolution is computed within the time-splitting [28] and fast Fourier-transformation techniques. The order parameter $\Psi(\mathbf{r}, t)$ is determined in the 3D cartesian grid. The requirement $\int_{+\infty}^{-\infty} dr^3 |\Psi(\mathbf{r}, t)|^2 = N$ is directly fulfilled by using an explicit unitary propagator. Reflecting boundary conditions are used throughout, but have no impact on the dynamics because of the harmonic confinement. In both static and time-dependent cases, only the order parameter with the lowest energy (chemical potential μ) is explicitly computed. No time-space factorization is used. The conservation of the total energy E and number of atoms N is controlled. Note that the Gross-Pitaevski equation is mathematically equivalent to the non-linear Schrödinger equation. In this sense, our approach is a counterpart of the time-dependent Hartree-Fock method for the system of interacting bosons.

The JO and MQST are studied in terms of the time-dependent normalized population imbalance z and phase difference θ ,

$$z(t) = \frac{N_L(t) - N_R(t)}{N}, \quad \theta(t) = \phi_R(t) - \phi_L(t), \quad (3)$$

where $N_{L,R}(t)$ are respectively populations of the left and right wells (with $N_L(t) + N_R(t) = N$) and $\phi_{L,R}(t)$ are the corresponding BEC phases. The populations read

$$N_j(t) = \int_{-\infty}^{+\infty} dr^3 |\Psi_j(\mathbf{r}, t)|^2 \quad (4)$$

with $j = L, R$ and $\Psi_L(\mathbf{r}, t) = \Psi(x \leq 0, y, z, t)$, $\Psi_R(\mathbf{r}, t) = \Psi(x \geq 0, y, z, t)$.

The phases $\phi_j(t)$ are defined as

$$\phi_j(t) = \arctan \frac{\gamma_j(t)}{\zeta_j(t)} \quad (5)$$

with the averages

$$\gamma_j(t) = \frac{1}{N_j} \int_{-\infty}^{+\infty} dr^3 \text{Im}(\Psi_j(\mathbf{r}, t)) |\Psi_j(\mathbf{r}, t)|^2, \quad (6)$$

$$\zeta_j(t) = \frac{1}{N_j} \int_{-\infty}^{+\infty} dr^3 \text{Re}(\Psi_j(\mathbf{r}, t)) |\Psi_j(\mathbf{r}, t)|^2. \quad (7)$$

Computation of the phase time evolution through arctan may be cumbersome. So we use (5) only for the static case while the time evolution is calculated through the phase

Table 1. Parameters of the procedure for the JO/MQST initial conditions. See text for detail.

N	$d, \mu\text{m}$		τ, ms		$q, \mu\text{m}$	
	JO	MQST	JO	MQST	JO	MQST
1000	0.25	0.5	4	8	5.2	5.2
3000	0.45	1.05	5	9	5.2	5.2
5000	0.62	1.35	5	5	5.2	6.6
10000	1.35	1.35	8	2	5.2	10.1

increments $\phi_j(t + \delta t) \approx \phi_j(t) + \delta\phi_j(t)$ for a small time step δt . Namely, we use

$$\delta\phi_j(t) = \sqrt{\frac{[\delta\gamma_j(t)]^2 + [\delta\zeta_j(t)]^2}{\gamma_j^2(t + \delta t) + \zeta_j^2(t + \delta t)}} \quad (8)$$

with $\delta\gamma_j(t) = \gamma_j(t + \delta t) - \gamma_j(t)$, $\delta\zeta_j(t) = \zeta_j(t + \delta t) - \zeta_j(t)$.

The calculations are performed for $N=1000$, 3000, 5000, and 10000 atoms. For all the cases, the initial population imbalance z_0 is 0.3 for JO and 0.6 for MQST [11, 12]. The initial phase difference is $\theta_0=0$ for both JO and MQST.

In most of the previous studies, the initial state is prepared as the lowest *non-stationary* state with the *constrained* z_0 in the *symmetric* trap, see, e.g. [8]. The constraint is reasonable for a weak coupling ($N=1000$ in our study) but may be questionable for SC where the chemical potential μ_x associated to the motion in x-direction approaches or even exceeds the barrier height. Besides, the constraint procedure deviates from the actual experimental initialization [11, 12] of the JO/MQST dynamics. Hence we use here, in addition to the constraint calculations, a more reliable and realistic initialization following [11, 12]. We start from the asymmetric trap produced from the symmetric one by a right-shift d of the barrier. The value of the shift is adjusted to provide the given z_0 in the lowest *stationary* state of the *asymmetric* trap. In some cases, an additional widening of the barrier, $q_0 \rightarrow q$, in the asymmetric trap is applied. Then the trap is rapidly (for a time τ) returned to the symmetric form and the JO/MQST time evolution starts.

The parameters of the procedure are given in Table 1. The return time τ is chosen to provide a reasonable initialization of JO/MQST. The calculations show that a too rapid return shakes the system and leads to a fussy and fragile JO/MQST. Instead, for too slow return, the equilibration process noticeably modifies z and θ from their initial values z_0 and θ_0 . Altogether, this procedure is more justified and realistic than the mere constraint. For $N=1000$, it fully reproduces formation of the initial conditions in the experiment [11, 12].

3. Results and discussion

3.1. Static interaction effect

In our study, we swap from weak to strong coupling (SC) and approach the crossover point by increasing the number of atoms N from 1000 to 10000. This results in rising the integral interaction effect and a subsequent growth of the chemical potential μ_x . Thus we naturally come from deeply sub-barrier to above barrier cases.

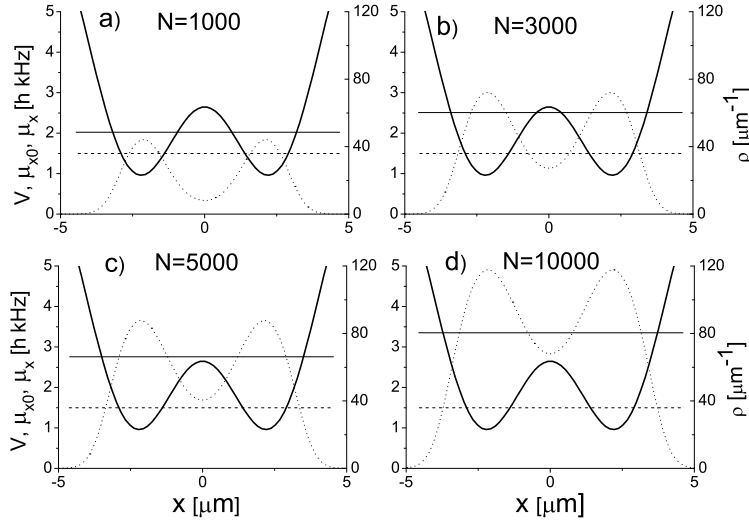


Figure 1. The double-well trap potential $V(x)$ (bold curve), the linear (without interaction) chemical potential μ_{0x} (dotted line), the non-linear (with interaction) chemical potential μ_x (solid line), and BEC density $\rho(x)$ (dotted curve) in the stationary states with $N_1 = N_2 = N/2$ for $N=1000$ (a), 3000 (b), 5000 (c), and 10000 (d).

This is demonstrated in Fig. 1 where the static BEC density $\rho(x)$ and chemical potential μ_x (for the motion in x-direction) are exhibited at different values of N and compared to the relevant trap potential $V_x(x) = m\omega_x^2 x^2/2 + V_0 \cos^2(\pi x/q_0)$. As mentioned above, the trap parameters are the same as in the experiment [11, 12]. The density

$$\rho(x) = \int_{-\infty}^{+\infty} dy dz |\Psi(x, y, z)|^2 \quad (9)$$

is determined from the solutions of (1) for interacting BEC.

Figure 1 shows that, for $N=1000$, the overlap of the left and right BECs is small. The ratio of the densities at their maxima ($x = \pm 2.2 \mu\text{m}$) and center of the trap ($x = 0$) is $\rho_m/\rho_c=5.1$. This is the case of the weak coupling used in the experiment [11, 12]. Increasing N results in rising the densities and larger overlap in the barrier region. At $N=10000$, we already have the SC case with $\rho_m/\rho_c=2$. Here the overlap of the left and right BECs cannot be neglected and the system should be treated with the *total* order parameter. At the same time, the left and right density bumps are still well distinctive. So a physical view of the system in terms of two (strongly coupled) BECs is

still reasonable and one may yet expect for the JO/MQST dynamics described by the relative variables z and θ .

To discriminate the sub-barrier and above-barrier cases, one should compare the chemical potential μ_x and the barrier height V_0 . For μ_x , only the motion in x -direction has to be taken into account. In the linear case ($g_0=0$), we straightforwardly get

$$\mu_{x0} = \mu_0 - \frac{\hbar}{2}(\omega_y + \omega_z) \quad (10)$$

Since $\omega_y + \omega_z = 2\omega_x$ [11, 12], the subtractive term in (10) is equal to $\hbar\omega_x$. The calculations give $\alpha = \mu_{x0}/\mu_0 = 3/4$, i.e. just x -motion mainly contributes to the total chemical potential μ_0 . This is because the barrier separates the harmonic x -confinement into two more narrow regions and thus effectively increases ω_x .

In the nonlinear case ($g_0 \neq 0$), the estimation of μ_x is straightforward for 1D system but complicated for 3D one. Here we roughly put $\mu_x = \alpha\mu$ where μ is the total *nonlinear* chemical potential. Hence we suppose that in the linear and nonlinear cases the relative contribution of x -motion to the chemical potential is the same.

Figure 1 compares the linear μ_{x0} and nonlinear μ_x to the barrier height V_0 . It is seen that μ_{x0} does not depend on N . It is always much lower than V_0 , thus leading to the deeply sub-barrier case. If the repulsive interaction is switched on, the nonlinear chemical potential μ_x rises with N . We see the sub-barrier case for $N = 1000$, the crossover region for $N=3000-5000$, and the above-barrier case for $N=10000$.

3.2. JO and MQST evolution

The evolution of JO and MQST with N is demonstrated in Figs. 2-3. In all cases, the initial ($t=0$) conditions are $z_0 = 0.3$, $\theta_0=0$ for JO and $z_0 = 0.6$, $\theta_0=0$ for MQST [11, 12]. Both the constraint technique (CT) and barrier-shift technique (BST) [11, 12], described in Sec. 2, are used for initialization of the dynamics. For the BST, the time τ when the asymmetric trap is fully reduced to the symmetric form is marked by a vertical line. It is seen that CT at $t=0$ and BST at $t = \tau$ give somewhat different z and θ . The larger N and τ (and thus the equilibration time), the more the difference. Nevertheless, the CT and BST usually initiate a similar (up to a constant time shift) dynamics, especially for JO. In what follows, we will mainly exam the BST results.

First of all, note that for $N=1000$ our calculations well reproduce the JO and MQST experimental data [11, 12]. Following Fig. 2 a),e), we obtain for JO the robust z - and θ -oscillations with the frequency $\omega_{JO} = 2\pi \times 23$ Hz which is close to the experimental value $\omega_{JO}^{\text{exp}} = 2\pi \times 25$ Hz. In Fig. 3a) for MQST, the calculations give z -oscillations around $\langle z \rangle = 0.6$ with the frequency $\omega_{MQST} = 2\pi \times 72$ Hz close to the experimental value $\omega_{MQST}^{\text{exp}} = 2\pi \times 78$ Hz. A small underestimation of the experimental frequencies can be caused by using in our calculations a smaller number of atoms, $N=1000$ instead of $N \approx 1150 \pm 150$ in the experiment. In Fig. 3e) for MQST, the computed θ linearly rises with the rate $\dot{\theta} = 2\pi \times 75$ Hz $\approx \omega_{MQST}$ similar to the experimental rate $2\pi \times 78$ Hz. The calculated oscillation amplitudes $\Delta z = z_{\text{max}} - z_{\text{min}} = 0.6$, $\Delta\theta = \theta_{\text{max}} - \theta_{\text{min}} = 1.4\pi$ for JO

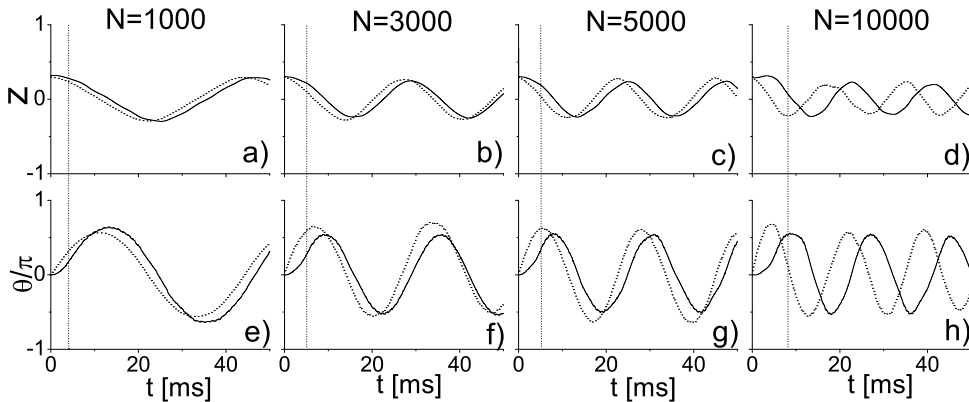


Figure 2. Time evolution of JO population imbalance z (upper plots) and phase difference θ (bottom plots) for $N=1000$, 3000 , 5000 , and 10000 , as indicated. The barrier-shift (solid line) and constraint (dotted line) techniques are used to initiate the evolution. For the barrier-shift case, the return time τ is marked by the vertical dash line. See text for more detail.

and $\Delta z=0.3$ for MQST also reproduce the experimental data. A good agreement of our results with the experiment [11, 12] proves high accuracy and realistic character of our method and justifies its application to the more sophisticated cases considered below.

The evolution of JO with N is exhibited in Fig. 2. It is seen that, despite a significant change in the conditions from $N=1000$ (weak coupling, sub-barrier transfer) through $N=3000-5000$ (significant coupling, crossover region) to $N=10000$ (strong coupling, above-barrier transfer), the JO keep the main features: oscillations of z and θ with the same frequency ω_{JO} around zero average values. The time shift between z and θ is about one-half a period. Amplitudes of the oscillations do not change with N . The evolution with N (or similarly with the interaction $U \sim g_0$ between BEC atoms) is mainly reduced to a growth of the frequency ω_{JO} . This trend is natural since the larger N , the higher the chemical potential μ_x and the larger the barrier penetrability K . Furthermore, the larger K , the higher ω_{JO} , as it should be in Rabi-like oscillations. Altogether we see that JO survive (with a higher frequency) even at SC and above-barrier transfer. The crossover region $N=3000-5000$ is passed monotonically.

Note that the above JO evolution is also supported by the weak-coupling arguments [9] though application of these arguments needs a word of caution. In the TMA weak-coupling picture for the interacting BEC [9], JO dynamics is driven by the interaction/coupling ratio $\Lambda = NU/K$. With increasing N , the interaction part NU grows linearly while the barrier penetrability K rises exponentially. Altogether, Λ falls with N which, following TMA calculations [9], should lead to decreasing ω_{JO} . Instead, our calculations demonstrate the opposite trend. The point is that our approach is a counterpart of the time-dependent Hartree-Fock method for boson systems, where the many-body problem for interacting bosons is reduced to one-body problem for a motion of a boson in an effective one-body potential involving the impact of the interaction. So the weak coupling arguments [9] should be used in the noninteracting limit where

$\omega_{\text{JO}} \propto K$. Hence the JO trend in Fig. 2.

In Figure 3, the evolution of MQST with N is demonstrated. As compared to JO, this evolution is more complicated and needs more time to be exhibited. Hence we use here the larger time interval 80 ms. Fig. 3 shows that MQST is transformed with N to JO from Fig. 2. Namely, at $N=1000$, there is an ordinary MQST in agreement with the experiment [11, 12]. At $N=3000-5000$, z -oscillations around $\langle z \rangle = 0.6$ are gradually reduced to slower oscillations around $\langle z \rangle = 0$ and, at $N=10000$, basically converge to JO in Fig. 2d). The linear evolution of θ is turned into JO-like oscillations around the average $\langle \theta \rangle = 2\pi$. Since the shift 2π is irrelevant, one actually gets the JO in Fig. 2h).

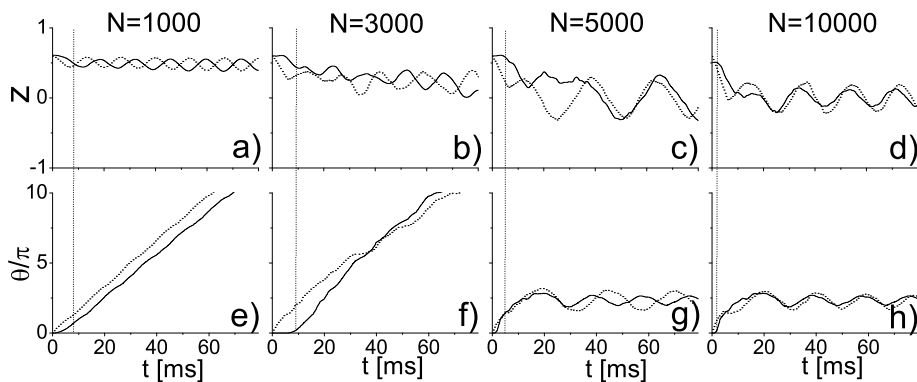


Figure 3. The same as in Fig. 2 but for MQST dynamics.

A similar MQST evolution was earlier obtained in the strong interaction limit for 1D BEC [26]. It was shown that at sufficiently strong interaction the amplitude of MQST z -oscillations starts to grow with NU_{1D} , thus leading to reappearance of tunneling between two wells. This effect was explained, within the modified TMA, by coupling the second and third modes. Our model takes into account all the modes and thus should cover the result [26] but now for 3D system. Actually, the transfer MQST \rightarrow JO in our calculations exhibits the similar effect: increasing the amplitude of z -oscillations and thus reappearance of the tunneling.

The most remarkable result of the present study is that, despite a significant overlap and strong coupling in the SC case, the left and right BECs in the trap still keep their individuality and accept the Josephson-like dynamics in terms of the relative variables, population imbalance z and phase difference θ . In particular, the JO dynamics obtained at a modest initial z_0 remains very regular and robust. This means that BEC interferometry and related processes may be successfully realized not only at weak coupling with a deeply sub-barrier transfer but also at SC with above-barrier transfer.

4. Summary

The dynamical evolution of coupled Bose-Einstein condensates (BEC) in a double well trap was investigated while modifying the system from a weak coupling case (small overlap of BECs, deeply sub-barrier transfer) to a strong coupling case (considerable overlap of BECs, above-barrier transfer). The evolution was driven by increasing the number N of BEC atoms and thus rising the total effect of the interaction between BEC atoms. The numerical analysis was performed by solving the 3-dimensional time-dependent Gross-Pitaevskii equation. Thus the two-mode and many other ordinary approximations were avoided. The main dynamical regimes, the Josephson oscillations (JO) and Macroscopic Quantum Self-Trapping (MQST), were inspected.

The calculations show that the JO successfully survive even at strong coupling but acquire a higher frequency. The MQST is destroyed and finally reduced to the same, though more fragile, high-frequency JO mode. Altogether we see that the Josephson-like dynamics certainly persists and remains robust at strong coupling. This means that, despite a strong overlap, the left and right BECs in the trap still keep their individuality and the relative variables, population imbalance z and phase difference θ , remain reliable. These findings show that BEC interferometry and related phenomena may be extended to the case of strong tunneling coupling, which opens a new avenue for further explorations.

Acknowledgments

The work was partly supported by the grants 11-02-00086 (RFBR, Russia), Université Paul Sabatier (Toulouse, France, 2009), and CNRS (2011). We are grateful to M. Melé-Messenger for useful discussions.

References

- [1] Petrick C J and Smith H 2002 *Bose-Einstein Condensation in Dilute Gases* (Cambridge: Cambridge University Press)
- [2] Pitaevskii L and Stringari S 2003 *Bose-Einstein Condensation* (Oxford: Oxford University Press)
- [3] Dalfovo F, Giorgini S, Pitaevskii L P and Stringari S 1999 *Rev. Mod. Phys.* **71** 463
- [4] Leggett A J 2001 *Rev. Mod. Phys.* **73** 307
- [5] Courteille P W, Bagnato V S and Yukalov V I 2001 *Laser Phys.* **11** 659
- [6] Gati R and Oberthaler M K 2007 *J. Phys. B: At. Mol. Opt. Phys.* **40** R61
- [7] Bloch I, Dalibard J and Zwerger W 2008 *Rev. Mod. Phys.* **80** 885
- [8] Melé-Messenger M, Juliá-Díaz B, Guilleumas M, Polls A and Sanpera A 2011 *New J. Phys.* **13** 033012
- [9] Smerzi A, Fantoni S, Giovanazzi S and Shenoy S R 1997 *Phys. Rev. Lett.* **79** 4950
- [10] Raghavan S, Smerzi A, Fantoni S and Shenoy S R 1999 *Phys. Rev. A* **59** 620
- [11] Albiez M, Gati R, Fölling J, Hunsmann S, Cristiani M and Oberthaler M K 2005 *Phys. Rev. Lett.* **95** 010402
- [12] Gati R, Albiez M, Fölling J, Hemmerling B and Oberthaler M K 2006 *Appl. Phys. B* **82** 207
- [13] Levy S, Lahoud E, Shomroni I and Steinhauer J 2007 *Nature* **449** 579
- [14] Nesterenko V O, Novikov A N, de Souza Cruz F F and Lapolli E L 2009 *Laser Phys.* **19** 616

- [15] Nesterenko V O, Novikov A N, Cherny A Y, de Souza Cruz F F and Suraud E 2009 *J. Phys. B: At. Mol. Opt. Phys.* **42** 235303
- [16] Schumm T *et al* 2005 *Nature Phys.* **1** 57
- [17] Esteve J, Gross C, Weller A, Giovanazzi S and Oberthaler M K 2008 *Nature* **455** 1216
- [18] Milburn G J, Corney J, Write E M and Walls D F 1997 *Phys. Rev. A* **55** 4318
- [19] Ananikian D and Bergeman T 2006 *Phys. Rev. A* **73** 013604
- [20] Ostrovskaya E A, Kivshar Y S, Lisak M, Hall B, Cattani F and Anderson D 2000 *Phys. Rev. A* **61** 031601
- [21] Lee C, Ostrovskaya E A and Kivshar Y S 2007 *J. Phys. B* **40** 4235
- [22] Streltsov A I, Alon O E and Cederbaum L S 2007 *Phys. Rev. Lett.* **99** 030402
- [23] Sakmann K, Streltsov A I, Alon O E and Cederbaum L S 2009 *Phys. Rev. Lett.* **103** 220601
- [24] Pitaevskii L P 1961 *Sov. Phys. JETP.* **13** 451; Gross E P 1961 *Nuovo Cim.* **20** 454
- [25] Olshanii M 1998 *Phys. Rev. Lett.* **81** 938
- [26] Juliá-Díaz B, Martorell J, Mele-Messeguer M and Polls A 2010 *Phys. Rev. A* **82** 063626
- [27] Blum V, Lauritsch G, Maruhn J A and Reinhard G P 1992 *J. Comput. Phys.* **100** 364
- [28] DeVries P L 1987 *AIP Conf. Proc.* **160** 269